Journal of Catalysis 273 (2010) 156–166

Contents lists available at ScienceDirect

Journal of Catalysis

journal homepage: www.elsevier.com/locate/jcat

Origin of the excellent catalytic activity of Pd loaded on ultra-stable Y zeolites in Suzuki–Miyaura reactions

Kazu Okumura *, Takuya Tomiyama, Shizuyo Okuda, Hiroyuki Yoshida, Miki Niwa

Department of Chemistry and Biotechnology, Graduate School of Engineering, Tottori University, 4-101 Koyama-cho Minami, Tottori 680-8552, Japan

ARTICLE INFO

Article history:
Received 17 April 2010
Revised 18 May 2010
Accepted 19 May 2010
Available online 26 June 2010

Keywords:
Suzuki–Miyaura reaction
Palladium
Ultra-stable Y zeolite
X-ray absorption fine structure
Acid property

ABSTRACT

Suzuki–Miyaura reactions were performed over Pd loaded on (ultra-stable Y) USY zeolites prepared by steam treatment of NH_4–Y. We found that the catalytic activity of Pd increased significantly with steam treatment of NH_4–Y when 6% H_2 was applied before and during the reactions. For instance, a TON of 13,000,000 was obtained in the reaction between bromobenzene and phenylboronic acid in 1.5 h. Pd K-edge and Pd L_3-edge X-ray absorption fine structure analyses revealed the formation of atomic Pd with a cationic character. The catalytic activity of Pd/USY prepared under different steam-treatment conditions was in good correlation with the strong Brønsted acid sites induced by the extra-framework Al. Based on the catalytic performance data, the structure of Pd, and acidic analysis of the support, atomic Pd anchored to the strong Brønsted acid sites of the USY zeolite was proposed to be the active species.

1. Introduction

Cross-coupling reactions, such as Suzuki–Miyaura and Mizoroki–Heck reactions, are important in the production of pharmaceuticals, organic electroluminescent devices, and liquid crystals [1–4]. Numerous Pd complexes, such as palladacycles [5] and *N*-heterocyclic carbine [6,7], have been developed for use in these reactions [8]. However, these Pd(0) or Pd(II) complexes cause difficulties in the synthesis and purification of the final product. Another class of catalysts for these reactions, namely heterogeneous catalysts, is easy to prepare and readily separated from the products. For this purpose, Pd has been supported on various materials, including active carbon [9], zeolites [10–13], double-layer hydroxides [14], modified silica [15–17], hydroxyapatite [18], and polymers such as dendrimers [19,20] and polyethylene glycol [21]. Among these supported catalysts, there are several reports on supported Pd catalysts that are nearly as active as the best homogeneous ones [13,14,22]. These highly active heterogeneous catalysts have been realized when well-dispersed active sites with a homogeneous structure are fabricated on supports. Moreover, well-dispersed metals having surface atoms with a low coordination number (CN) are anticipated to exhibit high activity; this behavior is different from that of a bulk-type catalyst. Zeolites have a large surface area and uniform micropores, which can accommodate dispersed metal clusters, leading to a high surface-to-volume ratio [23]. Using zeolites as supports for Pd is therefore expected to lead to high catalytic activity. Among the various zeolites, faujasite (FAU)-type zeolites are the most promising for use as a support for Pd because they have large supercage with diameters of ca. 1.3 nm. Indeed, we found that Pd loaded on ultra-stable Y (USY) zeolites exhibited excellent catalytic activity in a Suzuki–Miyaura reaction when H_2 was bubbled through the system prior to the reaction [24]. The reaction only took place when *o*-xylene and Pd ammine complexes were used as the solvent and the Pd precursor, respectively. The catalytic activity was improved significantly by continuously bubbling H_2 through the system during the reaction [22]. Pd K-edge extended X-ray absorption fine structure (EXAFS) analysis revealed the formation of atomic Pd species after H_2 bubbling in *o*-xylene. In addition to studying the active sites, it is important to obtain insights into the role of the support, taking into account that the catalytic performance of Pd varies significantly, depending on the type of support. Of particular interest is the USY zeolite, on which Pd exhibited extremely high activity in Suzuki–Miyaura reactions. However, little is known about the reason for the development of such a high activity in the Pd/USY catalyst. In general, USY zeolites are prepared by steam treatment of Y-type (FAU structure) zeolites ion exchanged with NH_4^+ cations (NH_4–Y) at temperatures of around 823 K [25]. The NH_4–Y steam treatment causes the formation of mesopores and the evolution of strong acid sites as a result of dealumination from the framework structure [26]. Tuning of the acid properties of USY is also possible by changing the steam-treatment conditions, i.e., temperature, time, and H_2O vapor concentration.

* Corresponding author. Fax: +81 857 31 5684.
E-mail address: okmr@chem.tottori-u.ac.jp (K. Okumura).

0021-9517/$ - see front matter © 2010 Elsevier Inc. All rights reserved.
doi:10.1016/j.jcat.2010.05.009

Here, we focused on the strong acid sites present in USY, with the aim of obtaining insight into the genesis of active species in Pd/USY which showed excellent catalytic performance in Suzuki–Miyaura reactions that was not realized on other kinds of supports including H–Y, ZSM-5, Mordenite, Al_2O_3, and active carbon [22]. This is because acid sites of zeolites played an important role in the determination of the dispersion of Pd, as proved primarily by in situ X-ray absorption fine structure (XAFS) studies [27–29]. The IR spectroscopy/MS spectrometry-temperature programmed desorption (IRMS-TPD) method of adsorbed NH_3 was used to study the acid properties of USY zeolites prepared under different steam-treatment conditions in detail. In this method, IR and MS work together to follow the thermal behavior of adsorbed and desorbed NH_3, respectively [30]. Using this method, information on the number and strength of acid sites is obtained simultaneously. The obtained data were correlated with catalytic performance coupled with XAFS data. Such a combined study enabled us to reveal the origin of the extremely high activity of Pd/USY catalysts.

2. Experimental methods

2.1. Catalyst preparation

Na–Y zeolite (320NAA) supplied by the Tosoh Corp., Tokyo, Japan was employed as the starting material for the preparation of USY. The Na–Y was ion exchanged three times with a solution of NH_4NO_3 (0.5 mol L^{-1}) at 353 K to give NH_4–Y. USY was prepared from NH_4–Y zeolites by treatment with H_2O vapor diluted with an N_2 flow. Typical concentration of H_2O vapor was 18 vol.% with an exception of steaming with 40 vol.%-H_2O. NH_4–Y (5 g) was placed in a quartz tube and treated with H_2O vapor for 1–10 h at 673–873 K. The total flow rate was 50 mL min^{-1}. The obtained USY was ion exchanged three times with NH_4NO_3 (0.5 mol L^{-1}) at 353 K to give NH_4–USY. The completion of ion exchange of H^+ with NH_4^+ was confirmed by TPD of NH_3, showing that 93% of H^+ had been replaced with NH_4^+. The NH_4–USY was then heated to 573 K in air to partially remove NH_3. Pd was then introduced to the calcined USY by an ion-exchange method using $Pd(NH_3)_4Cl_2$ solution (3.8×10^{-4} mol dm^{-3}; Aldrich, St. Louis, MO, USA) at room temperature (r.t.) [31]. The suspension was washed with deionized H_2O and dried in an oven at 323 K overnight. The Pd loading of all samples was 0.4 wt.%, as measured by inductive coupled plasma (ICP) analysis.

2.2. Catalytic reactions

Under typical conditions, bromobenzene (0.2 mol; Tokyo Kasei Chemicals Ltd., Japan), phenylboronic acid (0.32 mol; Tokyo Kasei Chemicals Ltd., Japan), K_2CO_3 (0.4 mol; Wako Chemicals Ltd., Osaka, Japan), *o*-xylene (solvent, 560 mL, Wako Chemicals Ltd., Osaka, Japan), and 0.4 wt.% Pd/USY catalyst (0.5 mg, Pd: 1.9×10^{-8} mol), weighed using an electronic microbalance, were used for the Suzuki–Miyaura reactions. A 6% H_2/94% Ar flow at a rate of 30 mL min^{-1} was introduced into the reactant solution using a glass capillary tube before and during the reaction, for 1 h at r.t. A three-necked flask (1 L) was placed in an oil bath, preheated to the required temperature, and subjected to vigorous stirring. The reaction was performed at 383 K. Suzuki–Miyaura reactions using chlorobenzene derivatives were performed under similar conditions, except for the use of DMF + H_2O (1.5 vol.%) and Cs_2CO_3 as the solvent and base, respectively. The reactions were performed in an Ar atmosphere. After reaction, the reaction mixture was cooled to r.t., and the solution was analyzed using a Shimadzu 2010 Gas Chromatograph equipped with an InertCap 5 (30 m) capillary column (Shimadzu Corp., Kyoto, Japan). Tridecane was used as the internal standard.

2.3. Pd K-edge and L_3-edge XAFS measurements and data analysis

Pd K-edge and Pd L_3-edge XAFS data were obtained from synchrotron radiation experiments performed at the BL01B1 station, with the approval of the Japan Synchrotron Radiation Research Institute (JASRI) (Proposal No. 2009B1107), and the BL10 station at the Ritsumeikan University SR Center, respectively. Pd K-edge XAFS data were collected in the quick mode; a Si(1 1 1) monochromator was continuously moved from 4.75° to 4.40° for 5 min. The beam size was 5 mm (horizontal) × 0.8 mm (vertical) at the sample position. For the Pd K-edge XAFS measurements, 6% H_2 was bubbled through a mixture of Pd/USY in *o*-xylene, and the treated Pd/USY was transferred to a plastic cell at r.t. without contact with air. The X-ray path length of the plastic cell was 2 cm. In the EXAFS analysis, oscillations were extracted by a spline smoothing method. The Fourier transformation of the k^3-weighted EXAFS oscillations and $k^3\chi(k)$ from the k space to the r space was carried out over the range 25–130 nm^{-1}. The inversely Fourier-filtered data were analyzed in the k range between 25 nm^{-1} and 130 nm^{-1} using a curve-fitting method. The inversely Fourier-filtered data were analyzed by the usual curve-fitting method, based on Eq. (1)

$$\chi^{(k)} = \sum N_j F_j(k) \exp(-2\sigma_j^2 k_j^2) \sin(2kr_j + \phi_j(k))/kr_j^2$$
$$k_j = (k^2 - 2m\Delta E_{0j}/\hbar^2)^{1/2} \quad (1)$$

where N_j, r_j, σ_j, and ΔE_{0j} represent the CN, the bond distance, the Debye–Waller factor, and the threshold energy difference between the reference and the sample, respectively. $F_j(k)$ and $\varphi_j(k)$ represent amplitude and phase shift functions, respectively. In the curve-fitting analysis, the empirical phase shift and the amplitude functions of Pd–O and Pd–Pd were extracted from the data obtained for PdO and Pd foils, respectively. CdS was used as the reference for Pd–Si/Al, as described in the literature [32].

For the collection of Pd L_3-edge XAFS data, the Pd/USY treated by bubbling 6% H_2 in *o*-xylene was transferred to a polyethylene bag (thickness = 10 μm) at r.t. Pd L_3-edge X-ray absorption near edge structure (XANES) data were recorded under He at atmospheric pressure in a fluorescence mode. A Ge(1 1 1) monochromator was moved stepwise from 37.3° to 35.0° for 30 min. The XAFS data were analyzed using the REX2000 (ver. 2.5) program developed by Rigaku Ltd., Tokyo, Japan. Error bars for each parameter in the EXAFS curve fitting were estimated by stepping each parameter, while optimizing the other parameter, with R factor becomes two times as its minimum value.

2.4. IRMS-TPD of NH_3

A Fourier-transform IR (FT-IR) spectrometer (Perkin-Elmer Spectrum-One; Perkin-Elmer, Waltham, MA, USA) and a mass spectrometer (Pfeiffer QME200; Pfeiffer, Asslar, Germany) were connected with a vacuum line kept at 3.3 kPa through which He was allowed to flow as the carrier (flow rate, 110 mL min^{-1}). An IR beam was transmitted to a self-compressed disk (5 mg and 10 mm in diameter). Details of the experimental apparatus have been described elsewhere [33]. After evacuation of the sample at 773 K, IR spectra were recorded before NH_3 adsorption at 10 K intervals from 373 to 773 K, while the temperature was increased at a rate of 10 K min^{-1} ($N(T)$, recorded). The bed temperature was then lowered to 373 K, at which point NH_3 was adsorbed at 13 kPa, and then gas-phase NH_3 was evacuated for 30 min. IR spectra were again measured at 10 K intervals from 373 to 773 K, while the temperature was raised ($A(T)$, recorded). The difference spectrum, i.e., $A(T) - N(T)$, was calculated at each temperature, and

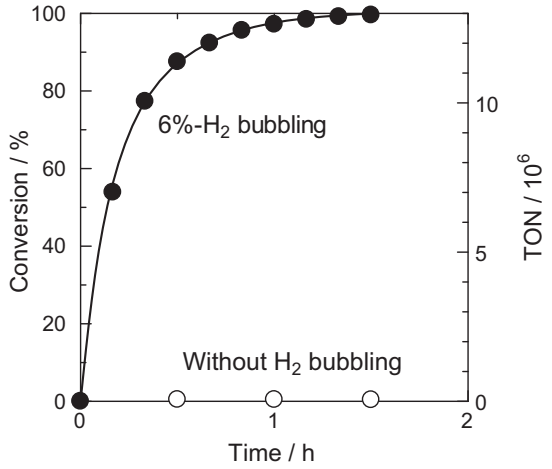

Fig. 1. Time course change in the conversion of bromobenzene over 0.4 wt.%-Pd/USY with or without 6%-H_2 bubbling. USY was prepared by steaming of NH_4–Y at 823 K for 10 h with 18% H_2O.

changes in IR absorptions were observed to identify the absorptions of NH_4^+ and NH_3 adsorbed on the surface. Changes in OH bands were also detected in the difference spectra as negative peaks. The difference spectra with respect to temperature, i.e., $-d(A(T) - N(T))/dT$, were calculated at selected band positions (referred to here as IR-TPD). In the present study, the area of IR absorption was quantified in the absorption range. The IR-TPD was compared with the MS-measured TPD of NH_3 (m/e, 16) to identify the nature of the adsorption site for the desorbed NH_3, i.e., a Lewis or a Brønsted acid site.

3. Results

3.1. Enhancement of the catalytic activity of Pd by steam treatment of NH_4–Y

3.1.1. Catalytic performance of Pd/USY in bromobenzene and bromonaphthalene derivatives

Suzuki–Miyaura coupling reactions of bromobenzene and bromonaphthalene derivatives were carried out over Pd loaded on USY prepared by steam treatment of NH_4–Y zeolite. In order to activate the Pd/USY catalyst, a 6%-H_2 flow at a rate of 30 mL min^{-1} was fed into the reactant solution using a glass capillary before and during the catalytic reactions. It should be emphasized that a small amount of 0.4 wt.% Pd/USY (0.5 mg) was used with respect to 0.2 mol of bromobenzene, which corresponds to 0.7×10^{-5} mol% Pd. We found that Pd/USY worked very efficiently in Suzuki–Miyaura reactions. Fig. 1 shows a typical change in the conversion of bromobenzene with time of the reaction with phenylboronic acid. Without the H_2-bubbling treatment, the activity of Pd/USY was almost negligible, with a turnover number (TON) of 30,000 being obtained. In marked contrast to this, the conversion of bromobenzene reached 88% in 30 min when H_2 bubbling was used. The reaction was completed in 1.5 h, and the Pd TON reached 13,000,000. The effect of the H_2 bubbling on the Suzuki–Miyaura reaction is therefore significant.

Table 1 lists representative data for reactions carried out in the presence of Pd/USY using various combinations of bromobenzene or bromonaphthalene derivatives and boronic acids carried out under 6%-H_2 bubbling. Very high TONs, higher than 2,400,000, were obtained with various bromobenzene derivatives in which the cross-coupling reaction proceeded almost quantitatively (entries 1– 5). The Pd/USY catalyst was also applicable to naphthalene

Table 1
Suzuki–Miyaura coupling reactions of aryl bromides catalyzed by 0.4 wt.%-Pd/USY activated with H_2 under in situ conditions.[a]
$Ar—Br + Ar'—B(OH)_2 \rightarrow Ar—Ar'$

Entry	Ar—Br	Ar′—B(OH)$_2$	Pd[b] (mol%)	Time (h)	Yield (%)	TON
1		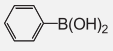	7.7×10^{-6}	1.5	99	13,000,000
2	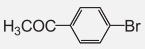	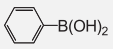	9.2×10^{-6}	1.5	99	11,000,000
3	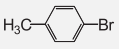	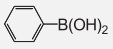	9.5×10^{-6}	3	96	11,000,000
4	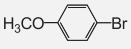	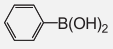	1.3×10^{-5}	6	89	8,900,000
5	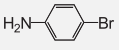	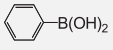	5.0×10^{-5}	18	83	2,400,000
6		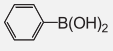	1.3×10^{-4}	1	99	760,000
7			2.2×10^{-3}	1	75	60,000
8	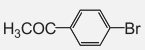		4.3×10^{-4}	1	99	230,000
9			9.2×10^{-4}	1	84	130,000
10	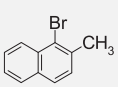		6.4×10^{-3}	1	78	20,000

[a] Typical reaction conditions (Entry 1): see Section 2.2. The scales of all reagents were changed, while the catalyst weight was fixed at 0.5–1.0 mg.
[b] Pd mol% with respect to the bromobenzene or bromonaphthalene derivatives used for reactions.

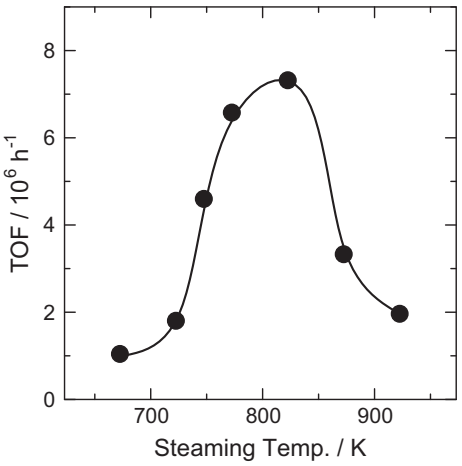

Fig. 2. TOFs plotted as a function of the steaming temperature for the preparation of USY in the coupling reaction between bromobenzene and phenylboronic acid. Steaming time for the preparation of USY was 1 h.

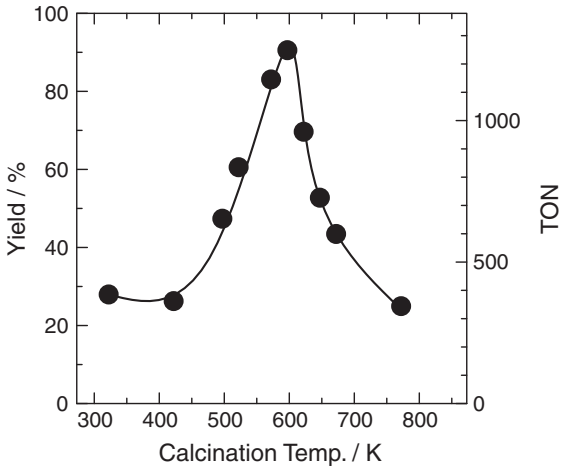

Fig. 3. Yield and TONs plotted as a function of the temperature for the calcination of NH_4–USY in the coupling reaction between 4-chloroacetophenone and phenylboronic acid. The TON was obtained at 10 min from the beginning of the reaction.

derivatives (entries 6–10), including reactions to give 1,1′-binaphthyl (entry 9).

Fig. 2 shows the turnover frequency (TOF) plotted as a function of the steam-treatment temperature for the preparation of USY in the reaction between bromobenzene and phenylboronic acid. TOFs were calculated based on the conversion of bromobenzene at 30 min from the beginning of the reaction and the amount of Pd present in Pd/USY. The TOF increased with increasing the steam-treatment temperature, with the highest activity being reached at 823 K. The activity declined on further increasing the steaming temperature. These data indicated the remarkable effect of steam-treatment conditions on the catalytic performance of Pd.

3.1.2. Catalytic performance of Pd/USY in chlorobenzene derivatives

Suzuki–Miyaura coupling reactions of chlorobenzene derivatives were carried out over Pd/USY in an Ar atmosphere. After screening of the solvents, we found that the addition of small amounts of H_2O (ca. 1.5 vol.%) to *N*,*N*-dimethylformamide (DMF) led to high Pd/USY catalyst activity. As shown in Table 2, we could obtain TON = 2000 and 1200 for the reactions between 4-chloroacetophenone or 4-chloronitrobenzene and phenylboronic acid, respectively, in 10 min. Unlike Pd/USY, Pd/NaX (NaX: Zeorum F-9, supplied by the Tosoh Corp., Tokyo, Japan) showed negligible activity in an Ar atmosphere (entry 3). A similar performance was observed in the reaction carried out in air.

The influence of the thermal treatment of NH_4–USY before Pd loading was then examined. Fig. 3 shows the yield of 4-acetylbiphenyl plotted as a function of the NH_4–USY calcination temperature in the reaction between 4-chloroacetophenone and phenylboronic acid. It can be seen from the figure that the yield is highly dependent on the NH_4–USY calcination temperature; the maximum yield was attained at 600 K. Similar data were obtained for the reaction using bromobenzene, as already reported [22]. The NH_4–Y steam-treatment temperature in the preparation of USY also affected the catalytic performance of Pd/USY. Fig. 4 shows the yield plotted as a function of steam-treatment temperature. The optimum temperature for the preparation of USY was 873 K, at which a yield of 94% and TON = 1300 was obtained.

Table 2
Suzuki–Miyaura coupling reactions of chlorobenzene derivatives catalyzed by 0.4 wt.%-Pd/USY.
Ar—Cl + Ph—$B(OH)_2$ → Ar—Ph

Entry	Catalyst	Ar–Cl	Pd[c] (mol%)	Yield (%)	TON
1[a]	USY	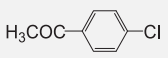	4.1×10^{-2}	81	2000
2[b]	USY	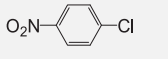	9.1×10^{-2}	92	1200
3[b]	NaX	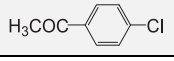	9.1×10^{-2}	0.3	4

[a] ArCl (5 mmol), $PhB(OH)_2$ (8 mmol), Cs_2CO_3 (10 mmol), DMF + H_2O (14 mL, H_2O: 1.5 vol.%). Temperature: 373 K. Time: 10 min, Ar atmosphere.
[b] ArCl (2.5 mmol), $PhB(OH)_2$ (4 mmol), Cs_2CO_3 (5 mmol), DMF + H_2O (7 mL, H_2O: 1.5 vol.%). Temperature: 373 K. Time: 10 min, Ar atmosphere.
[c] Pd mol% with respect to the chlorobenzene derivatives used for reactions.

3.2. Pd K-edge and Pd L_3-edge XAFS analysis of Pd/USY in *o*-xylene

Fig. 5 shows Pd K-edge $k^3\chi(k)$ EXAFS spectra and their Fourier transforms for $Pd(NH_3)_4Cl_2$/USY, measured with 6%-H_2 bubbling in *o*-xylene, in which USY was prepared by steam treatment at different temperatures. The color of the sample changed from white to black at 383 K. The EXAFS data of Pd/USY immersed in *o*-xylene were collected under in situ condition at 300 K after reduction with 6%-H_2 at 383 K using a plastic cell. The data for the curve-fitting analysis are summarized in Table 3. The Pd–Pd bond characteristic

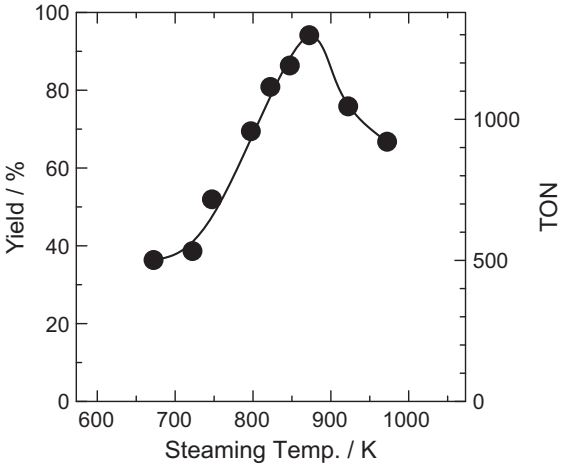

Fig. 4. Yield and TONs plotted as a function of the steaming temperature for the preparation of USY in the coupling reaction between 4-chloroacetophenone and phenylboronic acid. The TONs were obtained at 10 min from the beginning of the reaction.

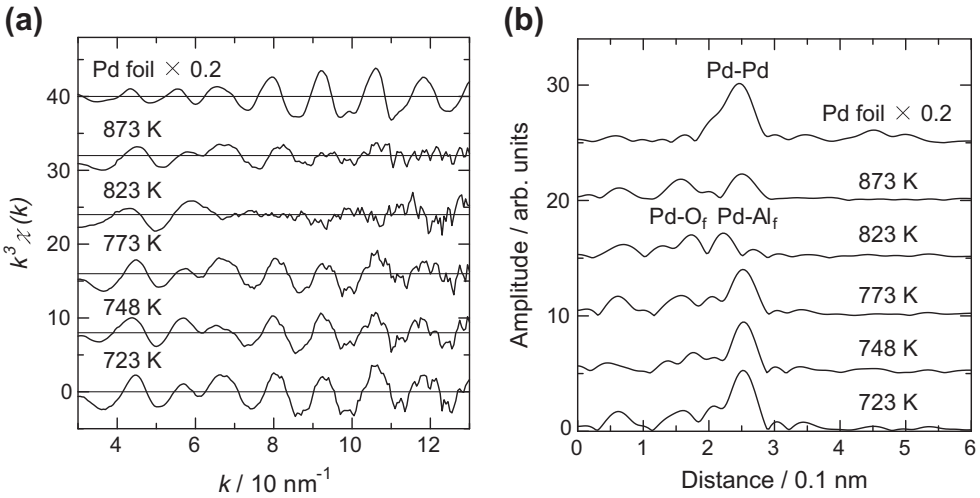

Fig. 5. Pd K-edge EXAFS: (a) $k^3\chi(k)$ and (b) their Fourier transforms of Pd loaded on USY prepared by steaming of NH_4–Y at different temperatures. Steaming time: 1 h, H_2O concentration: 18%.

Table 3
Curve-fitting analysis of Pd K-edge EXAFS data measured at r.t. for 0.4 wt.%-Pd loaded USY after the treatments with bubbling H_2 in *o*-xylene.

Temp.[a] (K)	Scatter	CN[b]	R[c] (nm)	ΔE_0[d] (eV)	DW[e] (nm)	R_f[f] (%)
723	Pd	4.3 ± 1.0	0.275 ± 0.001	5	0.0085	1.3
773	Pd	3.5 ± 0.7	0.276 ± 0.001	5	0.0087	1.7
823	O	1.1 ± 0.2	0.218 ± 0.001	−4	0.0074	1.7
	Al(Si)	1.0 ± 0.2	0.256 ± 0.001	2	0.0061	
Pd foil[g]	Pd	12	0.274			
PdO[g]	O	4	0.202			

[a] Steaming temperature of NH_4–Y for the preparation of USY zeolites.
[b] Coordination number.
[c] Bond distance.
[d] Difference in the origin of photoelectron energy between the reference and the sample.
[e] Debye–Waller factor.
[f] Residual factor.
[g] Data of X-ray crystallography.

of metallic Pd appeared in the samples prepared at 723–773 K with CNs of 3.5–4.3. The intensity of the Pd–Pd peak gradually decreased with increasing steam-treatment temperature, with the peak eventually vanishing at 823 K. In the spectrum of USY prepared at 823 K, two small peaks can be seen at 0.17 nm and 0.22 nm in the Fourier transforms. These bonds were assignable to Pd–O and to Pd–Al(Si) from the USY-zeolite framework, respectively, as reported earlier [22]. The Pd–O bond distance (0.218 nm) was longer than that of the covalent Pd–O bond (0.202 nm) in PdO, as shown in Table 3. This indicates the formation of mono-atomic Pd, because only the atoms present in the USY-zeolite framework were observed by EXAFS. On further increasing the temperature to 873 K, the Pd–O and Pd–Pd bonds appeared at 0.15 and 0.25 nm, respectively, implying that the Pd structure became inhomogeneous.

Information on the Pd valence state can be obtained in the Pd L_3-edge XANES region because electronic state of absorbing atom reflects on the spectra [34]. The Pd L_3-edge XANES data were recorded in an He flow (under atmospheric pressure), with the sample placed in a polyethylene bag 10 μm thick. Fig. 6 gives a comparison of the XANES region of Pd/USY, measured after bubbling with 6% H_2 in *o*-xylene, together with reference samples of Pd foil, $Pd(NH_3)_4Cl_2$, and K_2PdCl_6, which have oxidation states of 0, 2, and 4, respectively. The catalyst USY was prepared by the

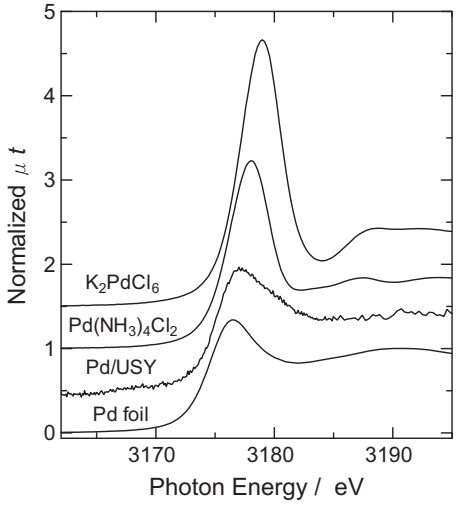

Fig. 6. Pd-L_3 edge XANES of Pd/USY treated with bubbling-H_2 in *o*-xylene at 383 K and reference samples.

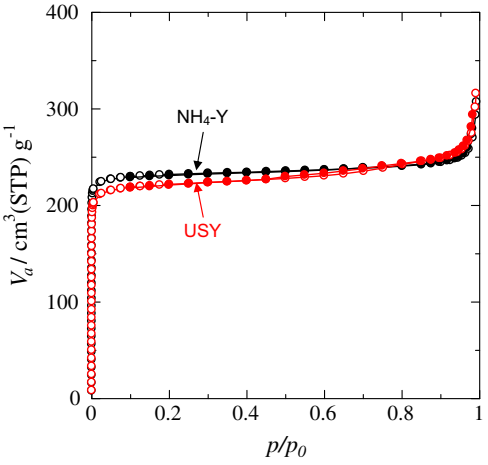

Fig. 7. N_2 adsorption isotherms of NH_4–Y and USY samples prepared by steaming at 823 K for 10 h with 18% H_2O. Open symbols: adsorption branches; Closed symbols: desorption branches.

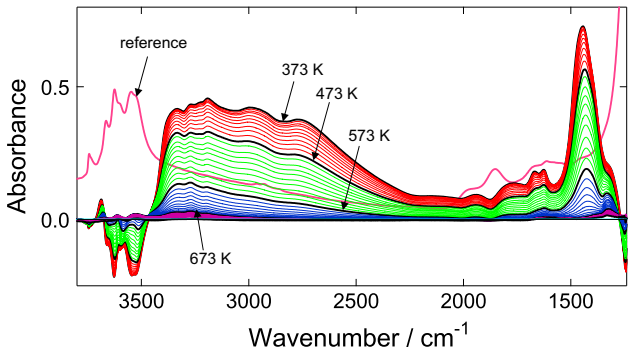

Fig. 8. Difference IR spectra measured on USY (steaming conditions: 18% H_2O at 823 K for 10 h) with adsorbed ammonia during the elevation of temperature from 373 to 773 K. Spectra were taken every 10 K. Bold lines show the spectra measured at 373, 473, 573, 673, and 773 K.

steam treatment at 823 K. It can be seen in the spectra of the reference samples that the intensities of the absorption peaks (white lines) increased, and their positions shifted to higher energies when the oxidation state of Pd increased. These white lines are attributed to the transition of the core electrons in $2p_{3/2}$ to the unoccupied 4*d* states above the Fermi level, and the intensities and positions of the white lines represent the valences and the energies of the core electrons, respectively [35,36]. The relative electron deficiency and ionic valence can be determined on the basis of the white line intensity [37,38]. It can be seen from the figure that the peak position and shape of the XANES for $Pd(NH_3)_4Cl_2$/USY are close to those of the Pd foil but shifted to a higher energy by about 0.6 eV. Judging from the intensity of the white line, the valence of Pd grafted on USY could be estimated to be +0.3. This means that the atomic Pd grafted on the USY support had a slight positive charge compared with Pd^0.

3.3. N_2 adsorption isotherms of NH_4–Y and USY supports

It is well known that steam treatment of NH_4–Y results in the formation of mesopores as a result of dealumination of the framework of Y-type zeolites [39,40]. Fig. 7 shows N_2 adsorption isotherms of NH_4–Y and the USY prepared by steam treatment with NH_4–Y (steam-treatment conditions: temperature 823 K; time 10 h; 18% H_2O). Although a slight change was observed after steam treatment with NH_4–Y compared with untreated NH_4–Y, no clear difference was found in USY. Moreover, mesopore formation was not seen in every USY sample; thus the possibility of mesopores participating in the Pd catalytic reaction is not plausible. The BET

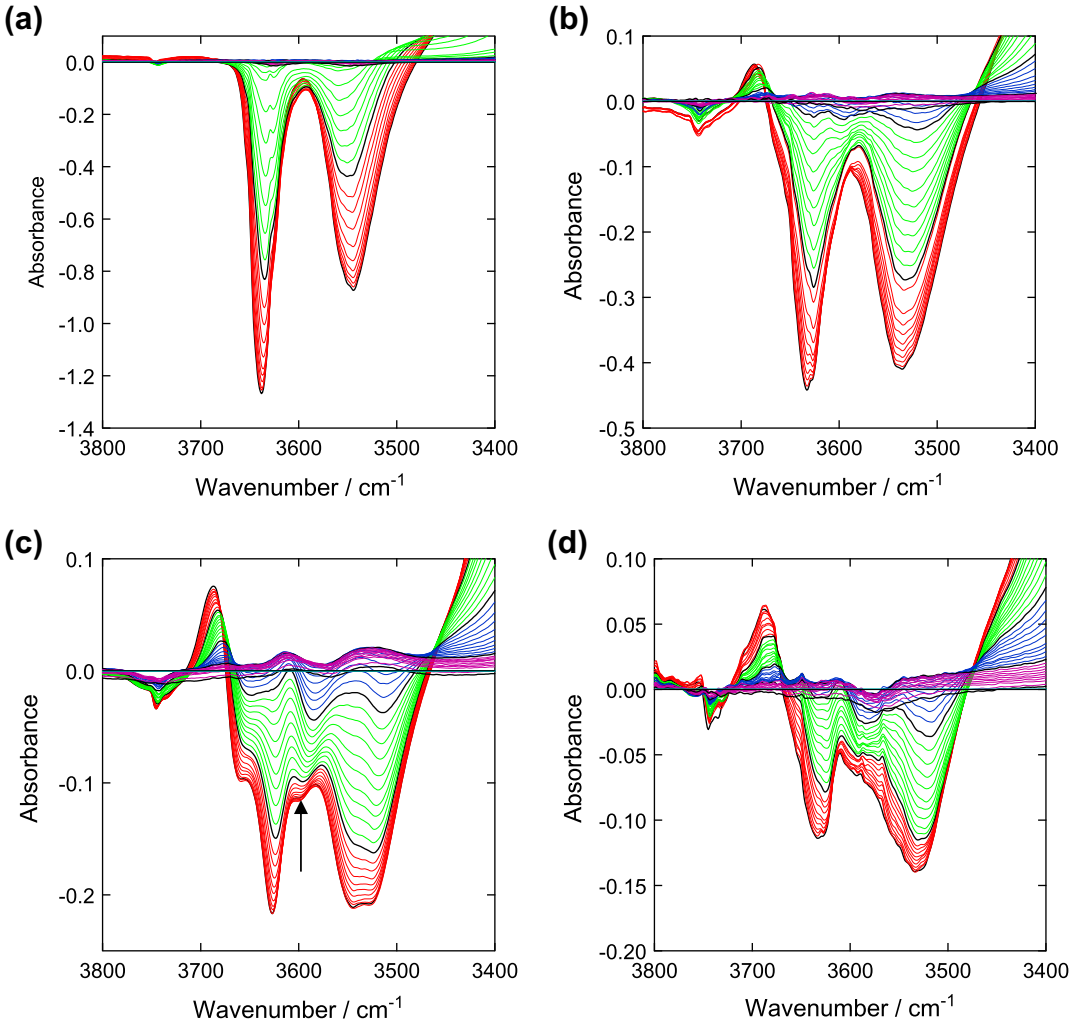

Fig. 9. Difference IR spectra measured on: (a) H–Y and (b–d) USY (prepared by steaming with 18% H_2O) with adsorbed ammonia during the elevation of temperature from 373 to 773 K. Spectra were taken every 10 K. Bold lines show the spectra measured at 373, 473, 573, 673, and 773 K. Steaming conditions: (a) untreated, (b) 773 K, 1 h, (c) 823 K, 10 h, and (d) 873 K, 1 h.

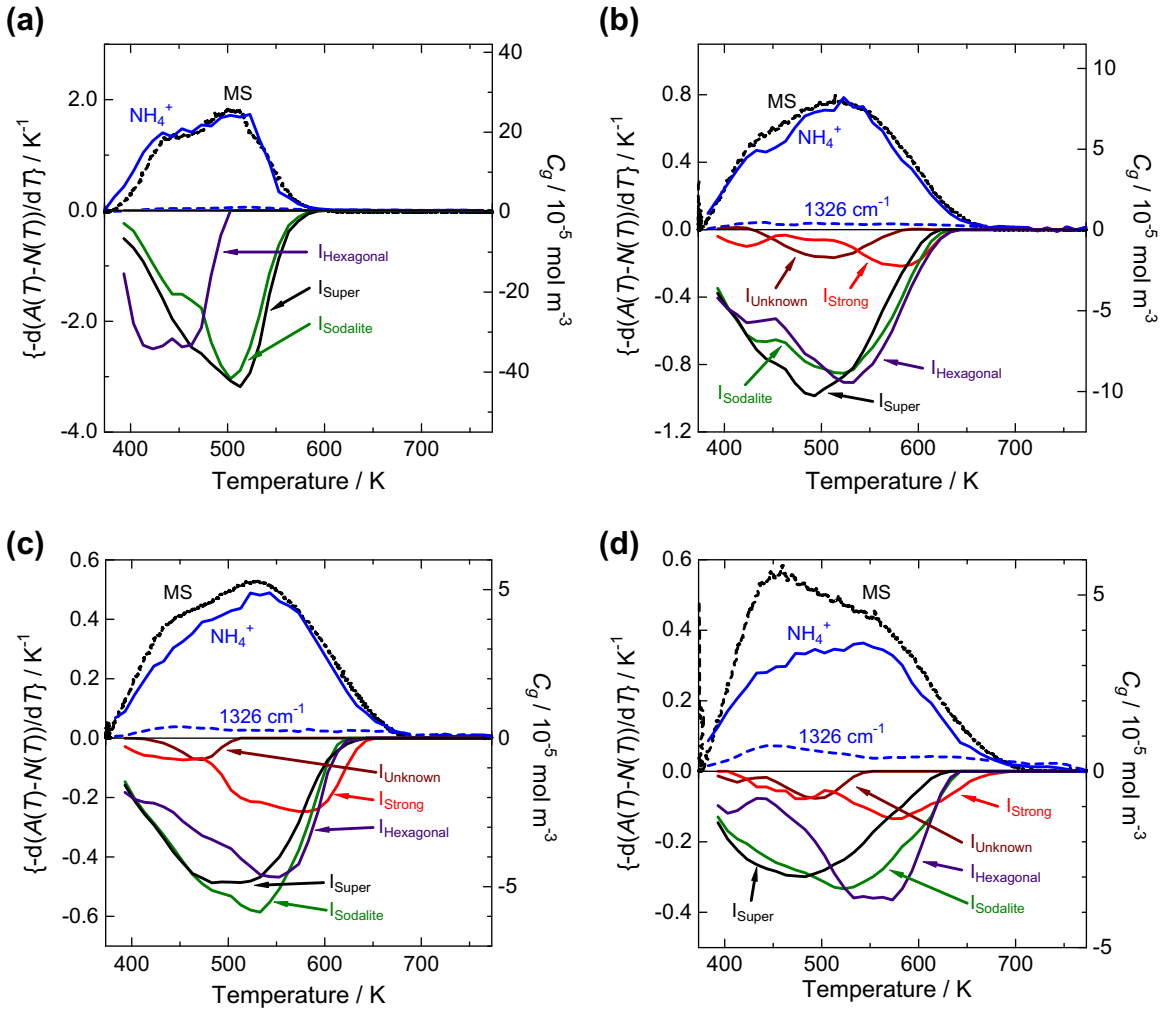

Fig. 10. IR-TPD of NH_4^+ and hydroxyl bands in the supercage, sodalite cage, strong acid site, hexagonal prism, and the unknown peak appeared at 3630 cm^{-1}, 3550 cm^{-1}, 3598 cm^{-1}, 3520 cm^{-1}, and 3609 cm^{-1}, respectively, together with MS-TPD as a comparison. Steaming conditions: (a) untreated, (b) 773 K, 1 h, 18% H_2O, (c) 823 K, 10 h, 18% H_2O, and (d) 873 K, 1 h, 18% H_2O.

surface areas of NH_4–Y and USY were calculated to be 710 and 690 $m^2\ g^{-1}$, respectively.

3.4. IRMS-TPD studies of acid sites in USY zeolites

Fig. 8 shows the difference IR-TPD spectra of USY (steam-treatment conditions: 18% H_2O at 823 K for 10 h) with adsorbed NH_3, as the temperature was raised from 373 to 773 K. A sharp absorption at 1432 cm^{-1}, ascribable to the NH_4^+ bending vibration, was clearly observed. Furthermore, a small absorption was observed at 1665 cm^{-1}, and this band was identified as weakly adsorbed NH_3. NH stretching vibrations also appeared in the broad region 3400–2500 cm^{-1}. A background spectrum measured at 373 K showed two OH bands at 3623 and 3550 cm^{-1}, which were identified as OH groups in the supercage and sodalite cage of the Y zeolite, respectively [41]. On NH_3 adsorption, these OH bands almost disappeared. The OH stretching region of the adsorbed NH_3, and the subsequent TPD, is enlarged in Fig. 9. The OH stretching region consisted of five kinds of OH groups: OH groups in the supercage (OH_{super}, 3630 cm^{-1}), unknown species ($OH_{unknown}$, 3609 cm^{-1}), sodalite cage ($OH_{sodalite}$, 3550 cm^{-1}), hexagonal prism ($OH_{hexagonal}$, 3520 cm^{-1}), and strong acid sides characteristic of USY (OH_{strong}, 3598 cm^{-1}) [42]. At high temperatures, a new negative band was seen at 3598 cm^{-1} (indicated by an arrow in Fig. 9c), which was not observed in the unmodified H–Y (Fig. 9a). The intensity of the OH_{strong} band increased with increasing temperature and NH_4Y steam-treatment time (Fig. 9b and c), so it is assumed that

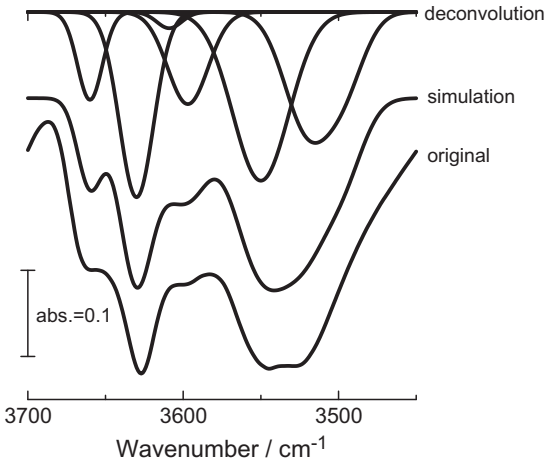

Fig. 11. Deconvolution of OH bands measured at 373 K into six components. Sum of them (simulation) was fitted well to the original drawn OH band in the difference spectrum. USY was prepared by steaming at 823 K, 10 h, with 18%-water vapor, corresponding to Figs. 8, 9c and 10c.

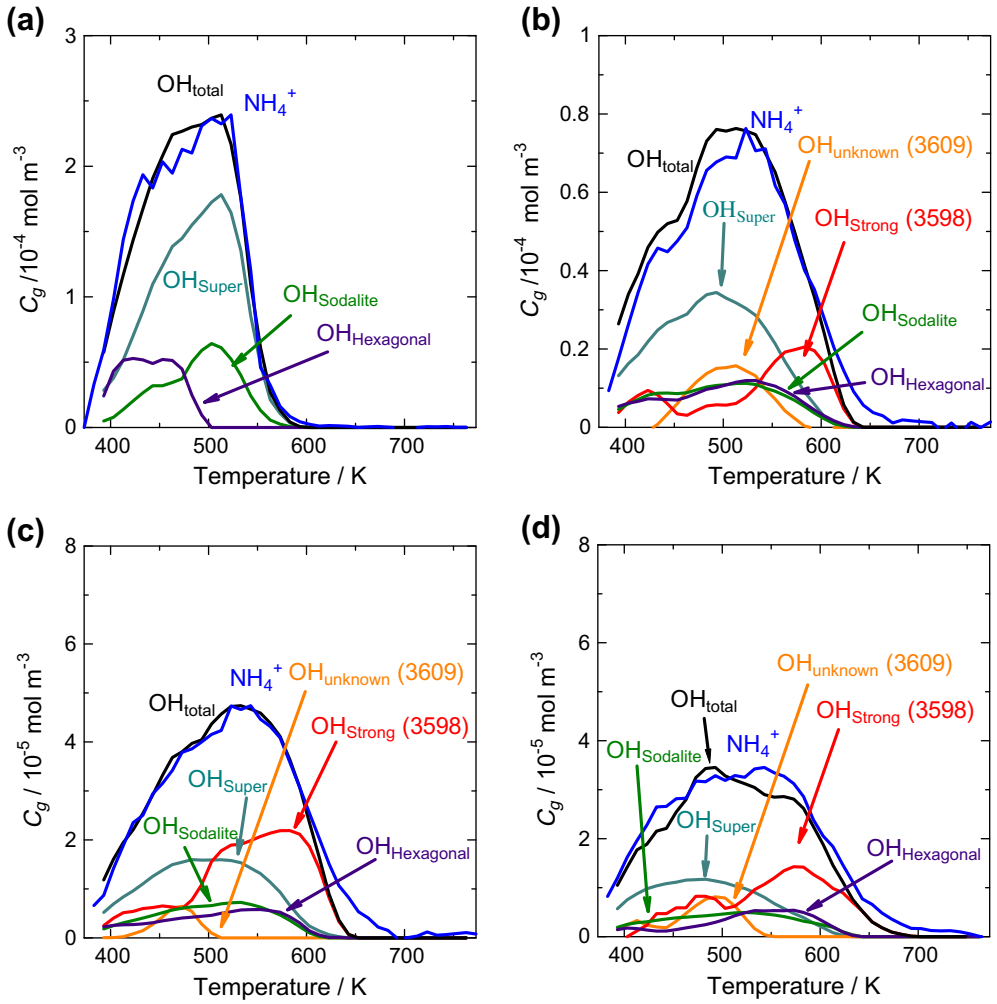

Fig. 12. Corrected IR-TPD of five kinds of OH groups, sum of them (I_0), and MS-TPD of ammonia to measure the amounts of Brønsted OH in the USY. Steaming conditions: (a) untreated, (b) 773 K, 1 h, 18% H_2O, (c) 823 K, 10 h, 18% H_2O, and (d) 873 K, 1 h, 18% H_2O.

this band was created as a result of the steam treatment. Excessive steam treatment at 873 K resulted in a decrease in the number of strong acid sites (Fig. 9d).

IR-TPD profiles of USY prepared under different steaming conditions were then calculated for OH bands and adsorbed ammonia species. Fig. 10 shows the IR-TPD spectra of H–Y and the USY prepared by steaming under different conditions. MS-measured TPD is also shown for a comparison in which desorption of NH_3 was found at ca. 500 K. Sum of the amounts of desorbed ammonia species shown by the IR-TPD curves must be equal to the MS-TPD of ammonia. In the calculation of IR-TPD, the absorbance area due to NH_4^+ was used for the quantification of adsorbed ammonia. On the other hand, the deconvolution of OH bands was made, as shown in Fig. 11, and the area of the OH band was quantified. The Brønsted OH bands should show a mirror-image correlation with that of NH_4^+. As a matter of fact, ammonia was desorbed at different temperatures from the OH species at ca. 470, 500, 530, 550, and 580 K arising from unknown species, OH groups in the supercage, sodalite cage, hexagonal prism, and newly created sites, respectively.

Then, the numbers of these OH groups were individually determined as follows: parameters, a_1–a_5, were determined by comparison of the IR-TPD of OH and MS-measured TPD of ammonia according to Eq. (2):

$$I_0 = a_1 I_1 + a_2 I_2 + a_3 I_3 + a_4 I_4 + a_5 I_5 \quad (2)$$

Here, I_1, I_2, I_3, I_4, and I_5 mean the intensity of IR-TPD of the OH bands at supercage, sodalite cage, the strong acid site, hexagonal prism, and unknown species, respectively, in which I_0 should agree with MS-TPD in size and shape. IR-TPD and MS-TPD have different units, but these are convertible because of the coincidence between IR-TPD of NH_4^+ and MS-TPD of NH_3 shown in Fig. 10. The number of total Brønsted acid sites was calculated from the desorbed amount of NH_3. The parameter a is a negative value and corresponds to the reciprocal of an extinction coefficient of the OH band. In other words, a is a parameter to cancel the difference in extinction coefficients in IR bands. By taking parameters as $a_1 = -3.4$, $a_2 = -9.2$, $a_3 = -9.2$, $a_4 = -1.3$, and $a_5 = -1.3$, I_0 could be compared with MS-TPD, as shown in Fig. 12. The amounts of acid sites determined by curve-fitting analysis are summarized in Table 4. The number of acid sites originating from supercage, sodalite cage, and hexagonal prism tended to decrease with increasing steam-treatment temperature and time. The maximum number of strong acid sites was reached at a steam-treatment temperature of 823 K (steaming time: 10 h). This trend was in good agreement with the catalytic performance in the reaction between bromobenzene and phenylboronic acid, in which maximum activity was attained at 823 K.

3.5. Correlation of acidic properties of USY and Pd catalytic activity

We then tried to correlate the number of acid sites for USY prepared under different steam-treatment conditions (temperature,

Table 4
Amount of acid sites in USY determined by NH_3 IRMS-TPD methods.

Steaming temp. (K)	Steaming time (h)	H_2O conc. (%)	OH_{total}[a] (mol kg^{-1})	OH_{super}[b] (mol kg^{-1})	$OH_{unknown}$[c] (mol kg^{-1})	OH_{strong}[d] (mol kg^{-1})	$OH_{sodalite}$[e] (mol kg^{-1})	$OH_{hexagonal}$[f] (mol kg^{-1})
773	1	18	0.86	0.37	0.11	0.14	0.12	0.12
823	0.2	18	0.85	0.37	0.14	0.12	0.12	0.10
823	1	40	0.82	0.23	0.03	0.13	0.08	0.10
823	5	18	0.59	0.21	0.06	0.16	0.08	0.08
823	10	18	0.56	0.19	0.03	0.21	0.07	0.06
873	1	18	0.34	0.11	0.04	0.10	0.05	0.04

[a] Total acids.
[b] Supercage.
[c] Unknown species.
[d] Strong acid sites.
[e] Sodalite cage.
[f] Hexagonal prism.

time, and H_2O concentrations) with the TOF in the reaction between bromobenzene and phenylboronic acid (Fig. 13). No obvious correlation was observed for the OH groups from supercage, sodalite cage, and hexagonal prism (Fig. 13b–d). In contrast, a linear relationship was obtained between TOF and the number of strong acid sites, i.e., OH groups appearing at 3598 cm^{-1} in the IR spectra (Fig. 13a), clearly indicating that the strong acid sites are related to the catalytic activity of Pd.

4. Discussion

We found that Pd/USY catalysts exhibited excellent activity in Suzuki–Miyaura reactions. This was achieved by choosing appropriate steam-treatment conditions for preparation of the USY support. Pd/USY could be used with various substrates, including bromobenzene, bromonaphthalene, and chlorobenzene derivatives. Bulky products, such as 1,1-binaphthyl, may be larger than

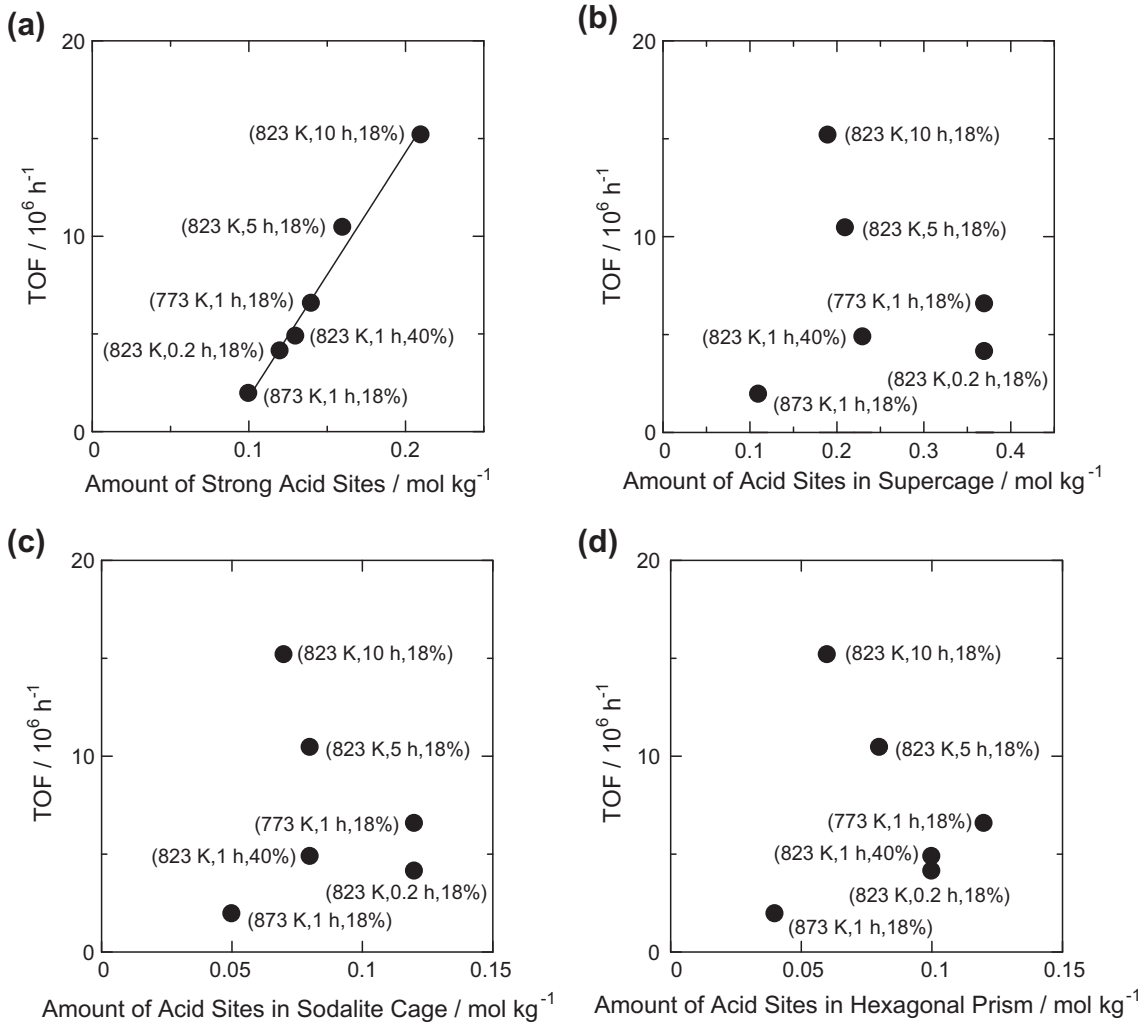

Fig. 13. Turnover frequencies plotted as a function of acid amount in: (a) strong acid sites, (b) supercages, (c) sodalite cages, and (d) hexagonal prisms. Numbers in parenthesis indicate the temperature, time and H_2O concentration for steaming.

the supercage in USY zeolites. Reactions involving bulky molecules are therefore thought to take place at the Pd located at the external USY surface. This is probably possible because USY has a relatively high external surface area (20 $m^2 g^{-1}$), as measured using the benzene-filled pore method [43].

Two possibilities are considered for the outstanding catalytic activity in Suzuki–Miyaura reactions of Pd loaded on USY. The first is the formation of mesopores in the USY support, which would assist transportation of reactants and products. This hypothesis may be ruled out because N_2 adsorption isotherms show that mesopore generation does not occur. Another possible mechanism is the stabilization of atomic Pd by the interaction with strong acid sites in the USY support. It is well known that USY zeolites have strong acid sites formed from extra-framework Al on steam treatment of NH_4–Y or Na–Y zeolites. The characteristic OH stretching band appeared at 3598 cm^{-1} in the IR spectra, accompanied by dealumination, which is ascribed to generation of strong acid sites on USY. The electron-withdrawing effect of the $AlOH^{2+}$ unit gives rise to formation of strong acid sites. In agreement with this assumption, Pd catalysis is sensitive to the steam-treatment temperature used in the preparation of USY from NH_4–Y; the highest activity is attained at 823 K. As can be seen from Fig. 13a, a linear relationship is obtained between the number of strong acid sites and the TOF. This means that the strong acid sites play an important role in the development of extremely high Pd catalytic activity. Atomic Pd is probably anchored on the USY support by interaction with strong acid sites, thus agglomeration of Pd is suppressed. In agreement with our studies, Xu et al. reported strong interactions between Pd and protons in zeolites [44]. Another possible role for the strong acid sites is the tuning of the electronic properties of Pd. In general, the Suzuki–Miyaura reaction is supposed to proceed through three steps: oxidative addition, transmetallation, and the reductive elimination [45]. It has been reported that the reductive elimination of products (biphenyl derivatives) is promoted by the electron-withdrawing effect of Pd [46]. The electronic effect of strong acid sites promotes the reductive elimination of products from the active center; the reaction is therefore greatly accelerated. Thus, we observe an interesting role for zeolite acidity, i.e., the interaction of Pd with the strong acid sites in zeolites induces extremely high catalytic activity in organic reactions.

Despite the formation of atomic Pd on the USY support, it is difficult to rule out the possibility of Pd leaching into the *o*-xylene, given the extremely small amount of Pd/USY (0.5–1.0 mg) used, and previous reports. Leadbeater [47], along with De Vries and Reetz [48], reported a very high activity for dissolved Pd at extremely low concentrations under specific conditions. In addition, Prockl reported that active Pd species dissolved in to a solvent during the reaction, but it was re-adsorbed on a zeolite supports after consumption of the substrates [49,50]. Therefore, another possibility is that Pd/USY provided the precursor for active species in the reactions. That is to say, the Pd complex leached inside the zeolite cage is the true active species, and it is possible that *o*-xylene plays a role in stabilization of this Pd species during the catalytic cycle.

We found that, in addition to the steaming conditions, the NH_4–USY calcination temperature also affected the catalytic performance of Pd (Fig. 3 and Ref. 24). The highest activity was obtained with NH_4–USY calcined at 573–600 K in the reactions using 4-chloroacetophenone and bromobenzene as substrates. According to the NH_3-TPD analysis, ca. half of the NH_4^+ cations remained on the USY support, compared with NH_4–USY [22]. It is assumed that the ion exchange of Pd^{2+} and zeolites takes place preferentially with the NH_4^+ cation rather than with H^+ [51]. Thus, Pd^{2+} can be introduced into sites on the USY zeolite of higher acid strength after calcination at 573 K. The Pd^{2+} was reduced with H_2 to give Pd^0. At the same time, protons remained on the ion-exchange sites. As a result, Pd^0 was grafted on the strong acid sites of the USY zeolite.

5. Conclusions

Suzuki–Miyaura reactions were carried out over Pd/USY catalysts. We found that the preparation conditions of the USY support influenced the catalytic performance of Pd. Very high TON values—higher than 10,000,000—were obtained after optimization of the steam-treatment conditions and the amount of NH_4^+ cations present in the USY. The Pd/USY catalysts could be used in various Suzuki–Miyaura reactions, including those using naphthalene and chlorobenzene derivatives. On the basis of the catalytic activity, Pd K-edge and Pd L_3-edge XAFS analyses, and IRMS-TPD studies, the active species was proposed to be the atomic Pd with partially cationic character, which was anchored to the strong acid sites induced by extra-framework Al species.

Acknowledgments

This research was partially supported by the Ministry of Education, Science, Sports and Culture, Grant-in-Aid for Scientific Research (C), 21560801, 2009-2011. The authors acknowledge Dr. Koji Nakanishi (Ritsumeikan University) for his technical support in the Pd-L_3 XANES measurements.

References

[1] A. Suzuki, A Modern Arene Chemistry: In the Suzuki Reaction with Arylboron Compounds in Arene Chemistry, Wiley, Weinheim, 2002. p. 53.
[2] A. Suzuki, J. Org. Chem. 576 (1999) 147.
[3] T. Mizoroki, K. Mori, A. Ozaki, Bull. Chem. Soc. Jpn. 44 (1971) 581.
[4] R.F. Heck, J.P. Nolley Jr., J. Org. Chem. 37 (1972).
[5] F. Bellina, A. Carpita, R. Rossi, Synthesis-Stuttgart (2004) 2419.
[6] E. Peris, R.H. Crabtree, Coord. Chem. Rev. 248 (2004) 2239.
[7] A.C. Hillier, G.A. Grasa, M.S. Viciu, H.M. Lee, C.L. Yang, S.P. Nolan, J. Organomet. Chem. 653 (2002) 69.
[8] E. Negishi, A. de Meijere, Handbook of Organopalladium Chemistry for Organic Synthesis, vol. 1, Wiley-VCH, New York, 2002. p. 39.
[9] F.X. Felpin, T. Ayad, S. Mitra, Eur. J. Org. Chem. (2006) 2679.
[10] L. Artok, H. Bulut, Tetrahedron Lett. 45 (2004) 3881.
[11] G. Durgun, O. Aksin, L. Artok, J. Mol. Catal. A 278 (2007) 189.
[12] A. Corma, H. Garcia, A. Leyva, Appl. Catal. A 236 (2002) 179.
[13] M. Choi, D.H. Lee, K. Na, B.W. Yu, R. Ryoo, Angew. Chem. Int. Ed. 48 (2009) 3673.
[14] B.M. Choudary, S. Madhi, N.S. Chowdari, M.L. Kantam, B. Sreedhar, J. Am. Chem. Soc. 124 (2002) 14127.
[15] C. Baleizao, A. Corma, H. Garcia, A. Leyva, Chem. Commun. (2003) 606.
[16] R.B. Bedford, U.G. Singh, R.I. Walton, R.T. Williams, S.A. Davis, Chem. Mater. 17 (2005) 701.
[17] C.M. Crudden, M. Sateesh, R. Lewis, J. Am. Chem. Soc. 127 (2005) 10045.
[18] K. Mori, T. Hara, M. Oshiba, T. Mizugaki, K. Ebitani, K. Kaneda, New J. Chem. 29 (2005) 1174.
[19] R. Narayanan, M.A. El-Sayed, J. Phys. Chem. B 108 (2004) 8572.
[20] L. Wu, B.L. Li, Y.Y. Huang, H.F. Zhou, Y.M. He, Q.H. Fan, Org. Lett. 8 (2006) 3605.
[21] J.W. Kim, J.H. Kim, D.H. Lee, Y.S. Lee, Tetrahedron Lett. 47 (2006) 4745.
[22] K. Okumura, H. Matsui, T. Tomiyama, T. Sanada, T. Honma, S. Hirayama, M. Niwa, Chemphyschem 10 (2009) 3265.
[23] D.W. Breck, Zeolite Molecular Sieves, Wiley, New York, 1974. p. 464.
[24] K. Okumura, H. Matsui, T. Sanada, M. Arao, T. Honma, S. Hirayama, M. Niwa, J. Catal. 265 (2009) 89.
[25] C.V. McDaniel, P.K. Maher, Zeolite Stability and Ultrastable Zeolites, American Chemical Society, Washington, 1976. p. 219.
[26] R.A. Beyerlein, C. ChoiFeng, J.B. Hall, B.J. Huggins, G.J. Ray, Top. Catal. 4 (1997) 27.
[27] K. Okumura, J. Amano, N. Yasunobu, M. Niwa, J. Phys. Chem. B 104 (2000) 1050.
[28] K. Okumura, T. Honma, S. Hirayama, T. Sanada, M. Niwa, J. Phys. Chem. C 112 (2008) 16740.
[29] K. Okumura, K. Kato, T. Sanada, M. Niwa, J. Phys. Chem. C 111 (2007) 14426.
[30] M. Niwa, K. Suzuki, N. Katada, T. Kanougi, T. Atoguchi, J. Phys. Chem. B 109 (2005) 18749.
[31] S. Bhatia, Zeolite Catalysis: Principles and Applications, CRC Press, Boca Raton, 1990. p. 239.
[32] K. Moller, D.C. Koningsberger, T. Bein, J. Phys. Chem. 93 (1989) 6116.
[33] M. Niwa, S. Nishikawa, N. Katada, Micropor. Mesopor. Mater. 82 (2005) 105.
[34] Z.L. Liu, K. Handa, K. Kaibuchi, Y. Tanaka, J. Kawai, Spectrochim. Acta, Part B 59 (2004) 901.
[35] D.C. Koningsberger, R. Prins, X-ray Absorption: Principles, Applications, Techniques of EXAFS, SEXAFS and XANES, Wiley, New York, 1988. p. 53.

[36] M. Benfatto, A. Bianconi, I. Davoli, L. Incoccia, S. Mobilio, S. Stizza, Solid State Commun. 46 (1983) 367.
[37] J.A. Horsley, J. Chem. Phys. 76 (1982) 1451.
[38] A.N. Mansour, J.W. Cook, D.E. Sayers, J. Phys. Chem. 88 (1984) 2330.
[39] A.H. Janssen, A.J. Koster, K.P. de Dong, J. Phys. Chem. B 106 (2002) 11905.
[40] A.H. Janssen, A.J. Koster, K.P. de Jong, Angew. Chem. Int. Ed. 40 (2001) 1102.
[41] F.R. Sarria, O. Marie, J. Saussey, M. Daturi, J. Phys. Chem. B 109 (2005) 1660.
[42] M. Niwa, K. Suzuki, K. Isamoto, N. Katada, J. Phys. Chem. B 110 (2006) 264.
[43] M. Inomata, M. Yamada, S. Okada, M. Niwa, Y. Murakami, J. Catal. 100 (1986) 264.
[44] L.Q. Xu, Z.C. Zhang, W.M.H. Sachtler, J. Chem. Soc. Faraday Trans. 88 (1992) 2291.
[45] N. Miyaura, A. Suzuki, Chem. Rev. 95 (1995) 2457.
[46] J.F. Hartwig, Inorg. Chem. 46 (2007) 1936.
[47] N.E. Leadbeater, Chem. Commun. (2005) 2881.
[48] M.T. Reetz, J.G. de Vries, Chem. Commun. (2004) 1559.
[49] S.S. Prockl, W. Kleist, M.A. Gruber, K. Kohler, Angew. Chem. Int. Ed. 43 (2004) 1881.
[50] S.S. Prockl, W. Kleist, K. Kohler, Tetrahedron 61 (2005) 9855.
[51] W.M.H. Sachtler, Catal. Today 15 (1992) 419.